HALL CURRENT EFFECTS ON UNSTEADY CONVECTIVE HEAT AND MASS TRANSFER IN A VERTICAL WAVY CHANNEL WITH THERMO DIFFUSION AND CHEMICAL REACTION

Dr. D. CHITTI BABU [1] **& Prof. D.R.V.PRASADA RAO** [2]

[1] **Department of Mathematics, Govt. College(A), Rajahmundry, A.P., INDIA**

[2] **Department of Mathematics, S.K.University,Anantapur, A.P., INDIA.**

ABSTRACT: In this paper we investigate the unsteady convective heat and mass transfer flow of a viscous electrically conducting fluid in a vertical wavy channel under the influence of an inclined magnetic fluid with thermo diffusion and chemical reaction. The unsteadiness in the flow is due to the traveling thermal wave imposed on the wall x=Lf(mz).The walls of the channels are maintained at constant concentrations. The equations governing the flow heat and concentration are solved by employing perturbation technique with the aspect ratio δ of the boundary temperature as a perturbation parameter. The velocity, temperature and concentration distributions are investigated for a different parameters. The rate of heat and mass transfer are numerically evaluated for different variations of the governing parameters.

Keywords: Heat, Mass transfer, Hall Currents, Convection, Porous media.

1. INTRODUCTION

The flow of heat and mass from a wall embedded in a porous media is a subject of great interest in the research activity due to its practical applications; the geothermal processes, the petroleum industry, the spreading of pollutants, cavity wall insulations systems, flat-plate solar collectors, flat-plate condensers in refrigerators, grain storage containers, nuclear waste management.

Rajesh et al[12] have discussed the time dependent thermal convection of a viscous, electrically conducting fluid through a porous medium in horizontal channel bounded by wavy walls. Kumar[7] has discussed the two-dimensional heat transfer of a free convective MHD(Magneto Hydro Dynamics) flow with radiation and temperature dependent heat source of a viscous incompressible fluid, in a vertical wavy channel. Recently Mahdy et al[8] have presented the Non-similarity solutions have been presented for the natural convection from a vertical wavy plate embedded in a saturated porous medium in the presence of surface mass transfer.

The study of heat and mass transfer from a vertical wavy wall embedded into a porous media became a subject of great interest in the research activity of the last two decades: Rees and Pop studied the free convection process along a vertical wavy channel embedded in a Darcy porous media, a wall that has a constant surface temperature or a constant surface heat flux. Cheng[3] for a power law fluid saturated porous medium with thermal and mass stratification. The influence of a variable heat flux on natural convection along a corrugated wall in a non-Darcy porous medium was established by Shalini and Kumar[20].

In all these investigations, the effects of Hall currents are not considered. However, in a partially ionized gas, there occurs a Hall current when the strength of the impressed magnetic field is very strong. These Hall effects play a significant role in determining the flow features. Sato[17], Yamanishi [24], Sherman and Sutton[22] have discussed the Hall effects on the steady hydromagnetic flow between two parallel plates. These effects in the unsteady cases were discussed by Pop[10]. Debnath[5] has studied the effects of Hall currents on unsteady hydromagnetic flow past a porous plate in a rotating fluid system and the structure of the steady and unsteady flow is investigated. Taking Hall effects in to account Krishna et al[6] have investigated Hall effects on the unsteady hydromagnetic boundary layer flow. Rao et al[11] have analyzed Hall effects on unsteady Hydromagnetic flow. Siva Prasad et al[23] have studied Hall effects on unsteady MHD free and forced convection flow in a porous rotating channel. Recently Seth et al[19] have investigated the effects of Hall currents on heat transfer in a rotating MHD channel flow in arbitrary conducting walls. Sarkar et al[16] have analyzed the effects of mass transfer and rotation and flow past a porous plate in a porous medium with variable suction in slip flow region. Anwar Beg et al[2] have discussed unsteady magnetohydrodynamics Hartmann-Couette flow and heat transfer in a Darcian channel with Hall current, ionslip,Viscous and Joule heating effects. Ahmed[1] has discussed the Hall effects on transient flow pas an impulsively started infinite horizontal porous plate in a rotating system. Shanti[21] has investigated effect of Hall current on mixed convective heat and mass transfer flow in a vertical wavy channel with heat sources. Leela[9] has studied the effect of Hall currents on the convective heat and mass transfer flow in a horizontal wavy channel under inclined magnetic field.

In this paper we investigate the unsteady convective flow of heat and mass transfer flow of a viscous electrically conducting fluid in a vertical wavy channel under the influence of an inclined magnetic fluid with thermo diffusion and chemical reaction. The unsteadiness in the flow is due to the traveling thermal wave imposed on the wall x=Lf(mz). The equations governing the flow heat and concentration are solved by employing perturbation technique with the aspect ratio δ of the boundary temperature as a perturbation parameter. The velocity, temperature and concentration distributions are investigated for a different values of G, D^{-1},M, m, N, So, α ,k and x+γt. The rate of heat and mass transfer are numerically evaluated for different variations of the governing parameters.

2. FORMULATION AND SOLUTION OF THE PROBLEM

We consider the unsteady flow of an incompressible, viscous electrically conducting fluid through a porous medium in a vertical channel bounded by two wavy walls under the influence of an inclined magnetic field of intensity Ho lying in the plane (y-z).The magnetic field is inclined at an angle α_1 to the axial direction k and hence its components are $(0, H_0 Sin(\alpha_1), H_0 Cos(\alpha_1))$.In view of the waviness of the wall the velocity field has components(u,0,w).The magnetic field in the presence of fluid flow induces the current($(J_x, 0, J_z)$.We choose a rectangular cartesian co-ordinate system O(x,y,z) with z-axis in the vertical direction and the walls at $x = \pm f(m z)$.

When the strength of the magnetic field is very large we include the Hall current so that the generalized Ohm's law is modified to

$$\bar{J} + \omega_e \tau_e \bar{J} x \bar{H} = \sigma(\bar{E} + \mu_e \bar{q} x \bar{H}) \qquad (2.1)$$

where q is the velocity vector. H is the magnetic field intensity vector. E is the electric field, J is the current density vector, ω_e is the cyclotron frequency, τ_e is the electron collision time,σ is the fluid conductivity and μ_e is the magnetic permeability. Neglecting the electron pressure gradient, ion-slip and thermo-electric effects and assuming the electric field E=0,equation (2.6) reduces

$$J_x - m H_0 J_z Sin(\alpha_1) = -\sigma \mu_e H_0 w Sin(\alpha_1) \qquad (2.2)$$

$$J_z + m H_0 J_x Sin(\alpha_1) = \sigma \mu_e H_0 u Sin(\alpha_1) \qquad (2.3)$$

where m= $\omega_e \tau_e$ is the Hall parameter.

On solving equations (2.2)&(2.3) we obtain

$$J_x = \frac{\sigma \mu_e H_0 Sin(\alpha_1)}{1 + m^2 H_0^2 Sin^2(\alpha_1)} (m H_0 Sin(\alpha_1) - w) \qquad (2.4)$$

$$J_z = \frac{\sigma \mu_e H_0 Sin(\alpha_1)}{1 + m^2 H_0^2 Sin^2(\alpha_1)} (u + m H_0 w Sin(\alpha_1)) \qquad (2.5)$$

where u, w are the velocity components along x and z directions respectively,

The Momentum equations are

$$\frac{\partial u}{\partial t} + u\frac{\partial u}{\partial x} + w\frac{\partial u}{\partial z} = -\frac{\partial p}{\partial x} + \mu(\frac{\partial^2 u}{\partial x^2} + \frac{\partial^2 u}{\partial z^2}) + \mu_e(-H_0 J_z Sin(\alpha)) - (\frac{\mu}{k})u \qquad (2.6)$$

$$\frac{\partial w}{\partial t}+u\frac{\partial w}{\partial x}+w\frac{\partial w}{\partial z}=-\frac{\partial p}{\partial z}+\mu(\frac{\partial^2 w}{\partial x^2}+\frac{\partial^2 w}{\partial z^2})+\mu_e(H_0 J_x Sin(\alpha_1))-(\frac{\mu}{k})w \qquad (2.7)$$

Substituting J_x and J_z from equations (2.4)&(2.5)in equations (2.6)&(2.7) we obtain

$$\frac{\partial u}{\partial t}+u\frac{\partial u}{\partial x}+w\frac{\partial u}{\partial z}=-\frac{\partial p}{\partial x}+\mu(\frac{\partial^2 u}{\partial x^2}+\frac{\partial^2 u}{\partial z^2})+ -\frac{\sigma\mu_e H_{0\,0}^2 Sin^2(\alpha_1)}{1+m^2H_0^2Sin^2(\alpha_1)}(u+mH_0 wSin(\alpha_1))-(\frac{\mu}{k})u \qquad (2.8)$$

$$\frac{\partial w}{\partial t}+u\frac{\partial w}{\partial x}+w\frac{\partial w}{\partial z}=-\frac{\partial p}{\partial z}+\mu(\frac{\partial^2 w}{\partial x^2}+\frac{\partial^2 w}{\partial z^2})- -\frac{\sigma\mu_e H_0^2 Sin^2(\alpha_1)}{1+m^2H_0^2Sin^2(\alpha_1)}(w-mH_0 uSin(\alpha_1))-(\frac{\mu}{k})w-\rho g \qquad (2.9)$$

The energy equation is

$$\rho C_p(u\frac{\partial T}{\partial x}+w\frac{\partial T}{\partial z}=k_f(\frac{\partial^2 T}{\partial x^2}+\frac{\partial^2 T}{\partial z^2})+Q \qquad (2.10)$$

The diffusion equation is

$$(\frac{\partial C}{\partial t}+u\frac{\partial C}{\partial x}+w\frac{\partial C}{\partial z}=D_1(\frac{\partial^2 C}{\partial x^2}+\frac{\partial^2 C}{\partial z^2})-k_1 C+k_{11}(\frac{\partial^2 T}{\partial x^2}+\frac{\partial^2 T}{\partial z^2}) \qquad (2.11)$$

The equation of state is

$$\rho-\rho_0=-\beta(T-T_o)-\beta^{\bullet}(C-C_o) \qquad (2.12)$$

The flow is maintained by a constant volume flux for which a characteristic velocity is defined as

$$q=\frac{1}{L}\int_{-Lf}^{Lf} w\,dx \qquad (2.13)$$

The boundary conditions are

u= 0 ,w=0 T= T_1 ,C=C_1 on $x=-f(mz)$ (2.14)

w=0, w=0, $T=T_2+(T_1-T_2)\sin(mz+nt)$, ,C=$C_2$ on $x=f(mz)$ (2.15)

On introducing the following non-dimensional variables $x' = x/L$, $z' = mz$, $t' = t\nu m^2$, ,

$$\psi' = \frac{\psi}{qL},\ \theta = \frac{T - T_2}{T_1 - T_2}, C' = \frac{C - C_2}{C_1 - C_2} \qquad (2.16)$$

the equation of momentum and energy in the non-dimensional form are

$$\nabla^4\psi - M_1^2\nabla^2\psi + \frac{G}{R}\left(\frac{\partial\theta}{\partial x} + N\frac{\partial C}{\partial x}\right) = \delta R\left(\frac{\partial\psi}{\partial z}\frac{\partial(\nabla^2\psi)}{\partial x} - \frac{\partial\psi}{\partial x}\frac{\partial(\nabla^2\psi)}{\partial z}\right) + \delta^2\frac{\partial(\nabla^2\psi)}{\partial t} \qquad (2.17)$$

$$\delta^2\frac{\partial\theta}{\partial t} + \delta PR\left(\frac{\partial\psi}{\partial x}\frac{\partial\theta}{\partial z} - \frac{\partial\psi}{\partial z}\frac{\partial\theta}{\partial x}\right) = \nabla^2\theta - \alpha\theta \qquad (2.18)$$

$$\delta^2\frac{\partial C}{\partial t} + \delta ScR\left(\frac{\partial\psi}{\partial x}\frac{\partial C}{\partial z} - \frac{\partial\psi}{\partial z}\frac{\partial C}{\partial x}\right) = \nabla^2 C - kC + \frac{ScSo}{N}\nabla^2\theta \qquad (2.19)$$

The corresponding boundary conditions are

$$\psi(f) - \psi(-f) = 1$$

$$\frac{\partial\psi}{\partial z} = 0, \frac{\partial\psi}{\partial x} = 0, \theta = 1, C = 1 \quad at\ x = -f(\delta z)$$

$$\frac{\partial\psi}{\partial z} = 0, \frac{\partial\psi}{\partial x} = 0, \theta = Sin(z + \gamma t)\ , C = 0 \quad at\ x = +f(z)$$

3. ANALYSIS OF THE FLOW

Introducing transformation

$$\eta = \frac{x}{f(\bar{z})} \qquad (3.1)$$

the governing equations are

$$F^4\psi - M_1^2 f^2 F^2\psi + \frac{Gf^3}{R}\left(\frac{\partial\theta}{\partial\eta} + N\frac{\partial C}{\partial\eta}\right) = \delta Rf\left(\frac{\partial\psi}{\partial\bar{z}}\frac{\partial(F^2\psi)}{\partial\eta} - \frac{\partial\psi}{\partial\eta}\frac{\partial(F^2\psi)}{\partial\bar{z}}\right) + \delta^2 f^2\frac{\partial(F^2\psi)}{\partial t} \qquad (3.2)$$

$$\delta^2 f^2\frac{\partial\theta}{\partial t} + \delta PRf\left(\frac{\partial\psi}{\partial\eta}\frac{\partial\theta}{\partial z} - \frac{\partial\psi}{\partial z}\frac{\partial\theta}{\partial\eta}\right) = F^2\theta - (\alpha f^2)\theta \qquad (3.3)$$

$$\delta^2 f^2\frac{\partial C}{\partial t} + \delta ScRf\left(\frac{\partial\psi}{\partial x}\frac{\partial C}{\partial z} - \frac{\partial\psi}{\partial z}\frac{\partial C}{\partial x}\right) = F^2 C - \gamma C + \frac{ScSo}{N}F^2\theta \qquad (3.4)$$

where

$$F^2 = \frac{\partial}{\partial \eta^2} + \delta^2 f^2 \frac{\partial}{\partial \bar{z}^2}$$

Assuming the aspect ratio δ of the boundary temperature to be small we take

$$\begin{aligned}
\psi(\eta,z,t) &= \psi_0(\eta,z,t) + \delta\psi_1(\eta,z,t) + \delta^2\psi_2(\eta,z,t) + \ldots\ldots\ldots\ldots \\
\theta(\eta,z,t) &= \theta_o(\eta,z,t) + \delta\theta_1(\eta,z,t) + \delta^2\theta_2(\eta,z,t) + \ldots\ldots\ldots\ldots \\
C(\eta,z,t) &= C_o(\eta,z,t) + \delta C_1(x,z) + \delta^2 C_2(\eta,z,t) + \ldots\ldots\ldots\ldots
\end{aligned} \tag{3.5}$$

Substituting (3.5) in equations (3.2)-(3.4) and equating the like powers of δ the equations and the respective boundary conditions to the zeroth order are

$$\frac{\partial^2\theta_0}{\partial\eta^2} - (\alpha f^2)\theta_0 = 0 \tag{3.6}$$

$$\frac{\partial^2 C_0}{\partial\eta^2} - k C_0 = -\frac{ScSo}{N}\frac{\partial^2\theta_0}{\partial\eta^2} \tag{3.7}$$

$$\frac{\partial^4\psi_0}{\partial\eta^4} - (M_1^2 f^2)\frac{\partial^2\psi_0}{\partial\eta^2} = -\frac{Gf^3}{R}\left(\frac{\partial\theta_0}{\partial\eta} + N\frac{\partial C_0}{\partial\eta}\right) \tag{3.8}$$

with

$$\begin{aligned}
&\psi_0(+1) - \psi_0(-1) = 1 \\
&\frac{\partial\psi_0}{\partial\eta} = 0,\ \frac{\partial\psi_0}{\partial\bar{z}} = 0, \quad \theta_0 = 1\ ,\ C_0 = 1 \quad at \quad \eta = -1 \\
&\frac{\partial\psi_0}{\partial\eta} = 0,\ \frac{\partial\psi_0}{\partial\bar{z}} = 0, \quad \theta_0 = \sin(z+\gamma t)\ ,\ C_0 = 0 \quad at \quad \eta = +1
\end{aligned} \tag{3.9}$$

and to the first order are

$$\frac{\partial^2\theta_1}{\partial\eta^2} - (\alpha f^2)\theta_1 = PRf\left(\frac{\partial\psi_0}{\partial\eta}\frac{\partial\theta_0}{\partial\bar{z}} - \frac{\partial\psi_0}{\partial\bar{z}}\frac{\partial\theta_0}{\partial\eta}\right) \tag{3.10}$$

$$\frac{\partial^2 C_1}{\partial\eta^2} - k C_1 = ScRf\left(\frac{\partial\psi_0}{\partial\eta}\frac{\partial C_0}{\partial\bar{z}} - \frac{\partial\psi_0}{\partial\bar{z}}\frac{\partial C_0}{\partial\eta}\right) - \frac{Sc\,So}{N}\frac{\partial^2\theta_1}{\partial\eta^2} \tag{3.11}$$

$$\begin{aligned}
\frac{\partial^4\psi_1}{\partial\eta^4} - (M_1^2 f^2)\frac{\partial^2\psi_1}{\partial\eta^2} &= -\frac{Gf^3}{R}\left(\frac{\partial\theta_1}{\partial\eta} + N\frac{\partial C_1}{\partial\eta}\right) + \\
&Rf\left(\frac{\partial\psi_0}{\partial\eta}\frac{\partial^3\psi_0}{\partial z^3} - \frac{\partial\psi_0}{\partial\bar{z}}\frac{\partial^3\psi_0}{\partial x\partial z^2}\right)
\end{aligned} \tag{3.12}$$

with

$$\psi_1(+1)-\psi_1(-1)=0$$
$$\frac{\partial\psi_1}{\partial\eta}=0,\quad \frac{\partial\psi_1}{\partial\bar{z}}=0,\quad \theta_1=0, C_1=0 \quad at \quad \eta=-1 \qquad (3.13)$$
$$\frac{\partial\psi_1}{\partial\eta}=0,\quad \frac{\partial\psi_1}{\partial\bar{z}}=0,\quad \theta_1=0\ .C_1=0 \quad at \quad \eta=+1$$

4. SOLUTIONS OF THE PROBLEM

Solving the equations(3.6)-(3.8) subject to the boundary conditions (3.9).we obtain

$$\theta_0=0.5\left(\frac{Ch(\beta_1\eta)}{Ch(\beta_1)}-\frac{Sh(\beta_1\eta)}{Sh(\beta_1)}\right)$$

$$C_0=a_5\left(\frac{Ch(\beta_2\eta)}{Ch(\beta_{12})}Ch(\beta_1)-Ch(\beta_1\eta)+a_8\left(\frac{Sh(\beta_2\eta)}{Sh(\beta_{12})}Sh(\beta_1)-Sh(\beta_1\eta)\right)+\right.$$
$$\left.+0.5\left(\frac{Ch(\beta_2\eta)}{Ch(\beta_{12})}-\frac{Sh(\beta_2\eta)}{Sh(\beta_{12})}\right)\right.$$

$$\psi_0=a_{17}Ch(\beta_3\eta)+a_{18}Sh(\beta_3\eta)+a_{19}\eta+a_{20}+f_2(\eta)$$

5. NUSSELT NUMBER and SHERWOOD NUMBER

The rate of heat transfer(Nusselt Number) on the walls has been calculated using the formula

$$Nu=\frac{1}{f(\theta_m-\theta_w)}\left(\frac{\partial\theta}{\partial\eta}\right)_{\eta=\pm1}$$

The rate of mass transfer(Sherwood Number) on the walls has been calculated using the formula

$$Sh=\frac{1}{f(C_m-C_w)}\left(\frac{\partial C}{\partial\eta}\right)_{\eta=\pm1}$$

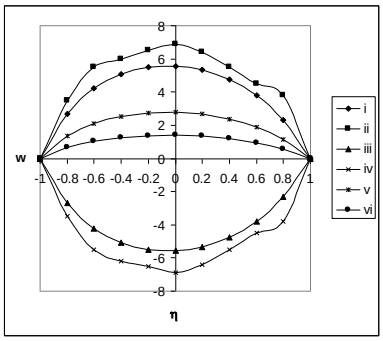

Fig. 1 : Variation of w with G, R

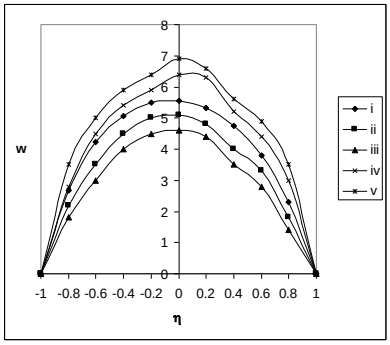

Fig. 2 : Variation of w with M, m

	I	II	III	IV	V	VI
G	10^3		$3x10^3$	-10^3	$3x10^3$	10 10^3
R	35		35	35	35	75 140

	I	II	III	IV	V
M	2	5	10	2	2
m	0.5	0.5	0.5	1.5	2.5

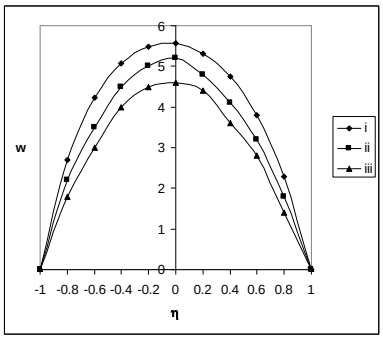

Fig. 3 : Variation of w with D^{-1}

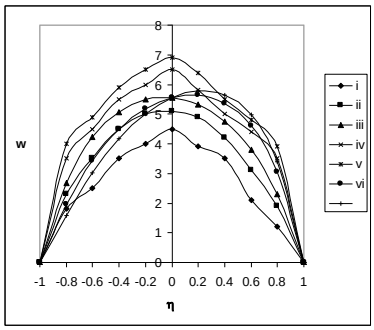

Fig. 4 : Variation of w with Sc, S_0

	I	II	III
D^{-1}	10^2	$2x10^2$	$3x10^2$

	I	II	III	IV	V	VI	VII
Sc	0.24	0.6	1.3	2.01	1.3	1.3	1.3
S_0	0.50	.5	0.5	0.5	1.0	-0.5	-1

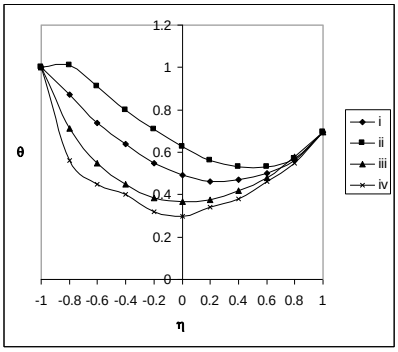

Fig. 5: Variation of θ with G

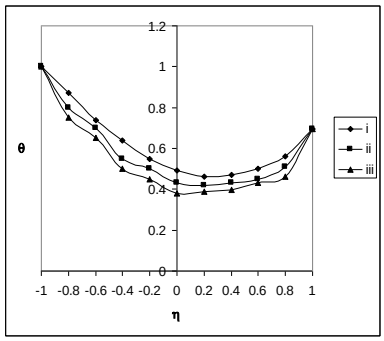

Fig. 6 : Variation of θ with R

	I	II	III	IV		I	II	III	
G	10^3	$3x10^3$	-10^3	$3x10^3$	R	35	75	140	

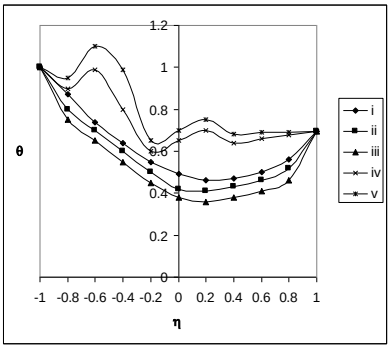

Fig. 7 : Variation of θ with M & m

		I	II	III	IV	V
M		2	5	10	2	2
m	0.5	0.5	0.5	1.5	2.5	

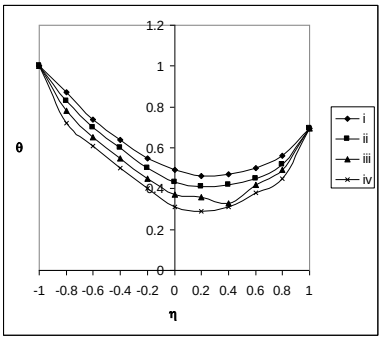

Fig. 8 : Variation of θ with K

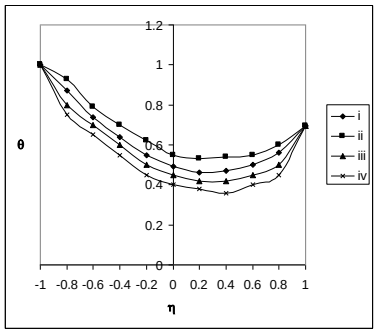

Fig. 9 : Variation of θ with N

	I	II	III	IV		I	II	III	IV
K	0.5	1.5	2.5	3.5	N	1	2	-0.5	-0.8

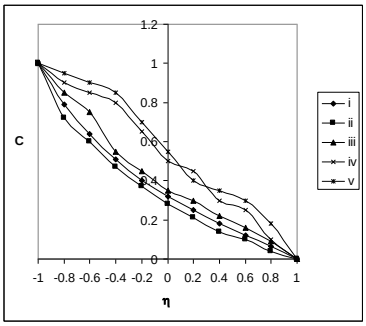

Fig. 10: Variation of C with M & m

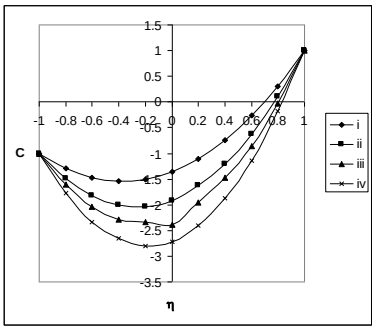

Fig. 11 : Variation of C with λ

	I	II	III	IV	V
M	2	5	10	2	2
m	0.5	0.5	0.5	1.5	2.5

	I	II	III	IV
λ	π/4	π/2	π	2π

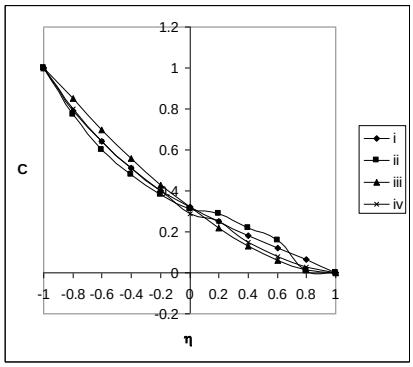

Fig. 12: Variation of C with x+γt

	I	II	III	IV
x+γt	π/4	π/2	π	2π

6.RESULTS AND DISCUSSION OF THE NUMERICAL RESULTS

In this analysis we investigate the effect of Hall currents on convective heat and mass transfer flow in a vertical wavy channel with thermo-diffusion and chemical reaction. The analysis has been carried out with Prandtl number P=0.71 and δ = 0.01.

The axial velocity(w) is shown in figures for different parametric values. Fig 1 represents the variation of w with G & R. It is found that the actual axial velocity is in the vertically upward direction and hence w<0 represents the reversal flow. w exhibits the reversal flow for G<0 and region of reversal flow enlarges with increase in |G|. |w| enhances with increase in |G| with maximum occurring at η = 0. An increase in Reynolds number R depreciates |w| in the entire flow region. Fig.2 & 3 represents the variation of w with M ,D^{-1}& m. It is found that higher the Lorentz force / lesser the permeability of the porous medium smaller |w| in flow region. An increase in the Hall parameter m enhances w in flow region. Fig.4 represents the variation of w with Sc & S_0. Lesser the molecular diffusivity larger |w| in the flow region. Also |w| enhances with increasing $S_0 > 0$ and reduces $|S_0|$ (<0). An increase in the chemical reaction parameter K. results in a depreciation in the axial velocity.

The non-dimensional temperature(θ)is shown in figures for different parametric values. Fig.5 represents θ with G. It is found that the actual temperature enhances with G>0 and reduces G<0.An increase in R results in a depreciation in the actual temperature(fig.6). The variation of θ with M & D^{-1} shows that higher the Lorentz force / lesser the permeability of the porous medium smaller u in the entire flow region. An increase in Hall parameter m results in an enhancement in the actual temperature (figs.7). An increase in the chemical reaction parameter k reduces the actual temperature everywhere(fig.8). The actual temperature enhances with N when the buoyancy forces act in the same direction and for the forces acting in opposite directions it depreciates in the flow region (fig.9).

The Concentration distribution(C) is shown in figures for different parametric values. An increase in M<5 reduces C and enhances with higher M>6.An increase in the Hall parameter menhances C in the flow region(fig.10). From fig.11 It is found that the actual concentration enhances with increase in λ. From fig.12 we find that the actual concentration depreciates with $x+\gamma t\leq\pi/2$ and for further higher $x+\gamma t=\pi$ we notice an enhancement and for still higher $x+\gamma t=2\pi$ the concentration depreciates in the entire flow region.

The rate of heat transfer (Nusselt Number(Nu))at the boundaries $\eta=\pm1$ is shown in tables 1-8 for different values of G, R, M, m, β, α, Sc, N, S_0, λ and $x+\gamma t$. It is found that the rate of heat transfer depreciates at both the walls with increase in |G|. Hihger the Lorentz force /lesser the permeability of the porous medum smaller |Nu| at $\eta=\pm1$. An increase in the Hall parameter m results in a depreciation in |Nu| at both the walls. |Nu| experiences an enhancement with increase in the strength of the heat source (tables 1 & 5). An increase in R reduces |Nu| at η = +1 for all G while at η = -1, |Nu| enhances in the heating case and reduces in the cooling case . Lesser the molecular diffusivity (Sc $\leq$1.3) smaller |Nu| at $\eta=\pm1$ and for further lowering of the diffusivity larger |Nu| at both the walls. The variation of Nu with Soret parameter S_0 shows that |Nu| reduces with S_0>0 and reduces with $|S_0|$ (<0) at $\eta=\pm1$ (tables 2 & 6). When the molecular buoyancy force dominates over the thermal buoyancy force the rate of heat transfer enhances at $\eta=\pm1$ when the buoyancy forces act in opposite directions and for the forces acting in the same direction |Nu| depreciates at η=-1 for all G while at η=+1, it enhances in the heating case and reduces in the cooling case. With reference to the chemical reaction parameter k we find that |Nu| depreciates at $\eta=\pm1$ with increase in k (tables 3 & 7). The variation of Nu with β reveals that higher the dilation of the channel walls lesser |Nu| and for further higher dilation larger |Nu| at $\eta=\pm1$. With respect to the inclination (λ) of the magnetic filed we find that an increase in $\lambda\leq\pi/2$ leads to a depreciation in |Nu| at $\eta=\pm1$ and for further higher $\lambda=\pi$, |Nu| reduces at η=-1 and at η=+1, it enhances for $|G|=10^3$ and reduces for $|G|=3x10^3$ and for still higher inclination of the magnetic field ($\lambda=2\pi$), |Nu| enhances at $\eta=\pm1$ in the heating case and reduces in the coding case. An increase in the phase $x+\gamma t\leq\pi/2$ reduces |Nu| at $\eta=\pm1$, and further higher $x+\gamma t\leq\pi$, it enhances at both the walls and for still higher $x+\gamma t\leq2\pi$, |Nu| reduces at η=-1 for all G. At η=+1, |Nu| enhances in the heating case and reduces in the cooling case (tables 4 & 8).

The rate of mass transfer (Sherwood number(Sh)) is shown in tables 9-16 for different parametric values. It is found that the rate of mass transfer reduces with G>0 and enhances with G<0 at both the walls. The variation of Sh with M & D^{-1} shows that higher the Lorentz force / lesser the permeability of the porous medium smaller |Sh| at $\eta=\pm1$ and for further higher Lorentz force / lowering of the permeability larger |Sh| at both the walls. With reference to heat source parameter α we find that the rate of mass transfer at η=-1 enhances with increase in $\alpha\leq4$ and reduces with higher $\alpha\geq6$, and at η=+1, it enhances with α for all G(tables 9 &13). An increase in R $\leq$70 leads to an enhancement in |Sh| at $\eta=\pm1$ and for higher R$\geq$140, we find an enhancement in |Sh| in the heating case and depreciation in the cooling case. Lesser the molecular diffusivity larger |Sh| and for further lowering of the diffusivity smaller |Sh| in heating case and larger in the cooling case and for still lowering of the molecular diffusivity larger |Sh| for G>0 and smaller for G<0. At $\eta=\pm1$, |Sh| enhances with increase in Sc$\leq$1.3 and for higher Sc$\geq$2.01, |Sh| reduces for all G. With respect to the Soret parameter S_0, we find that the rate of mass transfer at $\eta=\pm1$, enhances with increase in S_0>0 and depreciates with $|S_0|$(<0) and at η= -1, |Sh| enhances for G>0 and reduces for G<0 with increase in S_0>0 and a reversed effect is noticed in the behaviour of |Sh| with increase in $|S_0|$ (<0) (tables 10 & 14). When the molecular buoyancy force dominates over the thermal buoyancy force the rate of mass transfer enhances at both the walls when the buoyancy forces act in the same direction and for the forces acting in opposite directions, we notice a depreciate in |Sh| at $\eta=\pm1$.With reference to chemical reaction parameter k, we find that the rate of mass transfer enhances at η=+1 and at η=-1, larger in the heating case and lesser in the cooling case with increase in k$\leq$1.5 and for higher k$\geq$2.5, we find a depreciation in |Sh| at η=-1 (tables 11 & 15). Higher the dilation of the channel walls larger |Sh| at $\eta=\pm1$. The variation of Sh with λ shows that the rate of mass transfer at η=+1 depreciates with $\lambda\leq\pi/2$ and for further higher $\lambda=\pi$, |Sh| enhances and for still higher $\lambda=2\pi$, we notice a depreciation in |Sh|. At η=-1, |Sh| enhances with increase in $\lambda\leq\pi$ and depreciates with higher $\lambda=2\pi$. An increase in the phase $x+\gamma t\leq\pi$, leads to an enhancement in the rate of mass transfer at η=+1 and for higher $x+\gamma t=2\pi$, |Sh| enhances in the heating case and depreciates in the cooling case. At η = -1, |Sh| enhances with $x+\gamma t\leq\pi/2$, reduces with higher $x+\gamma t=\pi$ and again depreciates with still higher $x+\gamma t\leq2\pi$ (tables 12 & 16).

Table.1, **Average Nusselt Number(Nu) at η=1**

G/Nu	I	II	III	IV	V	VI	VII	VIII	IX
10^3	-0.5964	-0.0356	0.0042	-0.7417	-0.8421	-0.0269	0.0147	-0.5082	-0.7113
$3x10^3$	0.2110	0.1648	0.0022	0.0986	0.0322	0.2271	0.0998	0.9132	-0.0067
-10^3	1.1621	0.7281	0.0374	1.1582	1.1488	0.6911	0.2841	3.3368	4.4462
$-3x10^3$	0.7169	0.5016	0.0264	0.6868	0.6621	0.4767	0.1977	2.1611	2.7504

M	2	5	10	2	2	2	2	2	2
m	0.5	0.5	0.5	1.5	2.5	0.5	0.5	0.5	0.5
D^{-1}	10^2	10^2	10^2	10^2	10^2	$2x10^2$	$3x10^2$	10^2	10^2
α	2	2	2	2	2	2	2	4	6

Table.2

Average Nusselt Number(Nu) at η=1

G/Nu	I	II	III	IV	V	VI	VII	VIII	IX
10^3	0.2826	0.2596	-0.5964	1.3429	0.1978	-3.6047	15.1511	-0.6243	-0.6381
$3x10^3$	1.2348	1.0576	0.2110	1.4483	0.6543	-1.0254	-23.2527	0.2031	0.1990
-10^3	2.3653	2.1121	1.1621	1.6914	1.2786	0.8934	-0.3806	1.1652	1.1668
$-3x10^3$	1.9166	1.6851	0.7169	1.5836	0.9794	0.0397	-5.7365	0.7154	0.7146

Sc	0.24	0.6	1.3	2.01	1.3	1.3	1.3	2	2
So	0.5	0.5	0.5	0.5	1.0	-0.5	-1.0	0.5	0.5
R	35	35	35	35	35	35	35	70	140

Table.3

Average Nusselt Number(Nu) at η=1

G/Nu	I	II	III	IV	V	V
10^3	-0.5964	-1.8303	0.8926	1.15404	-0.5513	-0.6831
$3x10^3$	0.2110	-0.6412	1.2972	1.49144	0.1589	-0.0745
-10^3	1.1621	0.4592	2.0722	2.2367	1.1465	0.6925
$-3x10^3$	0.7169	-0.1069	1.7658	1.9531	0.7149	0.3191

N	1	2	-0.5	-0.8	1	1
k	0.5	0.5	0.5	0.5	1.5	2.5

Table.4

Average Nusselt Number(Nu) at η=1

G/Nu	I	II	III	IV	V	VI	VII	VIII	IX
10^3	0.3806	-0.5964	0.3622	-0.4586	-0.7004	-0.7553	-0.5341	1.8881	-3.5942
$3x10^3$	0.9984	0.2110	0.8481	0.2364	-0.0297	-0.0156	0.0796	2.2297	0.2601
-10^3	1.6901	1.1621	1.7738	1.0659	1.4632	1.3253	0.9939	1.5041	1.3309
$-3x10^3$	1.4073	0.7169	1.3751	0.7154	0.6895	0.6756	1.4012	1.2281	0.9856

β	0.3	0.5	0.7	0.5	0.5	0.5	0.5	0.5	0.5
λ	$\pi/4$	$\pi/4$	$\pi/4$	$\pi/2$	π	2π	$\pi/4$	$\pi/4$	$\pi/4$
$x+\gamma t$	$\pi/4$	$\pi/4$	$\pi/4$	$\pi/4$	$\pi/4$	$\pi/4$	$\pi/2$	π	2π

Table.5

Average Nusselt Number(Nu) at η=-1

G/Nu	I	II	III	IV	V	VI	VII	VIII	IX
10^3	1.3849	0.77732	0.0362	1.3956	1.3896	0.7289	0.2831	2.6893	2.9403
$3x10^3$	1.0401	0.3781	0.0053	1.0399	1.0214	0.5538	0.2176	2.4192	0.0029
-10^3	0.3849	0.3523	0.0202	0.3334	0.2964	0.3366	0.1462	1.7615	2.2881
$-3x10^3$	0.6947	0.4883	0.0255	0.6616	0.6345	0.4638	0.1913	2.0927	2.5308

M	2	5	10	2	2	2	2	2	2
m	0.5	0.5	0.5	1.5	2.5	0.5	0.5	0.5	0.5
D^{-1}	10^2	10^2	10^2	10^2	10^2	$2x10^2$	$3x10^2$	10^2	10^2
α	2	2	2	2	2	2	2	4	6

Table.6

Average Nusselt Number(Nu) at η=-1

G/Nu	I	II	III	IV	V	VI	VII	VIII	IX
10^3	3.2266	2.7475	1.3849	1.7633	1.4387	1.2157	-5.8173	1.3888	1.3911
$3x10^3$	2.4864	2.1213	1.0401	1.6424	1.2050	0.6032	-3.9546	1.0423	1.0434
-10^3	1.4452	1.2732	0.3849	1.4713	0.7434	-0.5458	-8.8465	0.3795	0.3768
$-3x10^3$	1.9718	1.7177	0.6947	1.5672	0.9646	-0.0391	-9.2754	0.6928	0.6919

Sc	0.24	0.6	1.3	2.01	1.3	1.3	1.3	2	2
So	0.5	0.5	0.5	0.5	1.0	-0.5	-1.0	0.5	0.5
R	35	35	35	35	35	35	35	70	140

Table.7

Average Nusselt Number(Nu) at η=-1

G/Nu	I	II	III	IV	V	VI
10^3	1.3849	0.4978	2.4888	2.6836	1.3556	0.7551
$3x10^3$	1.0401	0.2811	2.0144	2.1894	0.9038	0.4598
-10^3	0.3849	-0.4695	1.4718	1.6657	0.3931	0.0623
$-3x10^3$	0.6947	-0.1709	1.7891	1.9835	0.6941	0.2835

N	1	2	-0.5	-0.8	1	1
k	0.5	0.5	0.5	0.5	1.5	2.5

Table.8

Average Nusselt Number(Nu) at η=-1

G/Nu	I	II	III	IV	V	VI	VII	VIII	IX
10^3	2.2516	1.3849	2.0312	1.4479	1.0674	1.1677	1.1661	-3.3238	1.9616
$3x10^3$	1.7029	1.0401	1.6453	1.0391	0.8909	0.9268	0.8921	10.6042	1.3231
-10^3	0.8591	0.3849	1.2574	0.4044	0.3407	0.3161	0.3502	-4.1374	0.1796
$-3x10^3$	1.2593	0.6947	1.5093	0.6963	0.6595	0.6464	1.6234	-1.7547	0.7034
β	0.3	0.5	0.7	0.5	0.5	0.5	0.5	0.5	0.5
λ	$\pi/4$	$\pi/4$	$\pi/4$	$\pi/2$	π	2π	$\pi/4$	$\pi/4$	$\pi/4$
$x+\gamma t$	$\pi/4$	$\pi/4$	$\pi/4$	$\pi/4$	$\pi/4$	$\pi/4$	$\pi/2$	π	2π

Table.9

Sherwood Number(Sh)at η=1

G/Nu	I	II	III	IV	V	VI	VII	VIII	IX
10^3	-0.7591	-0.7431	-0.7977	-0.7621	-0.7638	-0.7426	-0.7427	-5.0153	2.1899
$3x10^3$	-0.7061	-0.6913	-0.9826	-0.7109	-0.7133	-0.6926	-0.6925	-2.0975	-4.3214
-10^3	-0.8378	-0.8215	-0.8913	-0.8411	-0.8431	-0.8211	-0.8224	1.2638	0.4967
$-3x10^3$	-0.9439	-0.9273	-1.0188	-0.9476	-0.9498	-0.9269	-0.9306	0.0784	-0.0601
M	2	5	10	2	2	2	2	2	2
m	0.5	0.5	0.5	1.5	2.5	0.5	0.5	0.5	0.5
D^{-1}	10^2	10^2	10^2	10^2	10^2	$2x10^2$	$3x10^2$	10^2	10^2
α	2	2	2	2	2	2	2	4	6

Table.10

Sherwood Number(Sh) at η=1

G/Nu	I	II	III	IV	V	VI	VII	VIII	IX
10^3	0.0426	0.6367	-0.7591	-0.2145	-0.7952	-0.7146	-0.6854	-0.7744	-0.7825
$3x10^3$	0.0284	1.4846	-0.7061	-0.2143	-0.7473	-0.6964	-0.6581	-0.7434	-0.7655
-10^3	-0.0854	0.0705	-0.8378	-0.2146	-0.8536	-0.7229	-0.7094	-0.8167	-0.8069
$-3x10^3$	-0.0629	-0.0180	-0.9439	-0.2147	-0.9214	-0.7337	-0.7343	-0.8584	-0.8247
Sc	0.24	0.6	1.3	2.01	1.3	1.3	1.3	2	2
So	0.5	0.5	0.5	0.5	1.0	-0.5	-1.0	0.5	0.5
R	35	35	35	35	35	35	35	70	140

Table.11

Sherwood Number(Sh) at η=1

G/Nu	I	II	III	IV	V	VI
10^3	-0.7591	-0.7785	-0.6653	-0.6668	-0.8748	-2.1335
$3x10^3$	-0.7061	-0.6845	-0.6893	-0.7093	-0.8219	-1.6136
-10^3	-0.8378	-0.9727	-0.6447	-0.6337	-0.5321	-0.6754
$-3x10^3$	-0.9439	-1.4574	-0.6275	-0.6087	-0.7101	-1.1003

N	1	2	-0.5	-0.8	1	1
k	0.5	0.5	0.5	0.5	1.5	2.5

Table.12

Sherwood Numbeer(Sh) at η=1

G/Nu	I	II	III	IV	V	VI	VII	VIII	IX
10^3	-0.6421	-0.7591	-0.8226	-0.7547	-0.7659	-0.7652	1.0481	-0.8018	-0.7028
$3x10^3$	-0.5954	-0.7061	-0.7746	-0.7048	-0.7154	-0.7148	-0.8479	-0.8850	-0.6597
-10^3	-0.7071	-0.8378	-0.9235	-0.8332	-0.8452	-0.8446	-0.1875	-0.7245	-0.7655
$-3x10^3$	-0.7923	-0.9439	-1.0708	-0.9391	-0.9523	-0.9516	-0.7071	-0.6736	-0.8353

β	0.3	0.5	0.7	0.5	0.5	0.5	0.5	0.5	0.5
λ	π/4	π/4	π/4	π/2	π	2π	π/4	π/4	π/4
x+γt	π/4	π/4	π/4	π/4	π/4	π/4	π/2	π	2π

Table.13

Sherwood Number(Sh) at η=-1

G/Nu	I	II	III	IV	V	VI	VII	VIII	IX
10^3	-0.3474	-0.3354	-0.3969	-0.3498	-0.3508	-0.3350	-0.3376	-11.1605	5.8291
$3x10^3$	-0.2213	-0.2204	-0.5277	-0.2225	-0.2232	-0.2192	-0.2239	-1.3599	-3.8313
-10^3	-0.4796	-0.4563	-0.5229	-0.4841	-0.4869	-0.4556	-0.4547	5.3912	4.2534
$-3x10^3$	-0.7293	-0.6891	-0.7675	-0.7373	-0.7423	-0.6872	-0.6837	2.7849	3.7468

M	2	5	10	2	2	2	2	2	2
m	0.5	0.5	0.5	1.5	2.5	0.5	0.5	0.5	0.5
D^{-1}	10^2	10^2	10^2	10^2	10^2	$2x10^2$	$3x10^2$	10^2	10^2
α	2	2	2	2	2	2	2	4	6

Table.14

Sherwood Number(Sh)at η=-1

G/Nu	I	II	III	IV	V	VI	VII	VIII	IX
10^3	0.1931	0.6101	-0.3474	-0.3656	-0.3576	-0.1865	-0.1881	-0.3825	-0.4011
$3x10^3$	0.1374	2.2417	-0.2213	-0.3651	-0.2816	-0.2446	-0.1833	-0.3043	-0.3534
-10^3	0.0331	0.2677	-0.4796	-0.3658	-0.4361	-0.1671	-0.2031	-0.4344	-0.4132
$-3x10^3$	0.0885	0.3166	-0.7293	-0.3662	-0.5475	-0.1159	-0.2056	-0.5412	-0.4670

Sc	0.24	0.6	1.3	2.01	1.3	1.3	1.3	2	2
So	0.5	0.5	0.5	0.5	1.0	-0.5	-1.0	0.5	0.5
R	35	35	35	35	35	35	35	70	140

Table.15

Sherwood Number(Sh) **at η=-1**

G/Nu	I	II	III	IV	V	VI
10^3	-0.347	-0.428	-0.110	-0.097	-1.693	-0.046
$3x10^3$	-0.221	-0.194	-0.165	-0.191	-0.121	0.9232
-10^3	-0.479	-0.770	-0.079	-0.047	3.9618	2.1843
$-3x10^3$	-0.729	-1.884	-0.036	0.0134	1.6317	1.6412

N	1	2	-0.5	1	1
k	0.5	0.5	0.5	1.5	2.5

Table.16

Sherwood Numbewr(Sh) at η=-1

G/Nu	I	II	III	IV	V	VI	VII	VIII	IX
10^3	-0.2024	-0.3474	-0.4539	-0.3437	-0.3526	-0.3518	2.9986	-0.2284	-0.2612
$3x10^3$	-0.1360	-0.2213	-0.2541	-0.2209	-0.2237	-0.2236	-0.4180	-0.2759	-0.1832
-10^3	-0.2672	-0.4796	-0.7017	-0.4733	-0.4901	-0.4892	0.8928	-0.2318	-0.3234
$-3x10^3$	-0.3863	-0.7293	-1.2301	-0.7185	-0.7476	-0.7461	2.7507	-0.2009	-0.4471
β	0.3	0.5	0.7	0.5	0.5	0.5	0.5	0.5	0.5
λ	$\pi/4$	$\pi/4$	$\pi/4$	$\pi/2$	π	2π	$\pi/4$	$\pi/4$	$\pi/4$
$x+\gamma t$	$\pi/4$	$\pi/4$	$\pi/4$	$\pi/4$	$\pi/4$	$\pi/4$	$\pi/2$	π	2π

REFERENCES

1. Ahmed N and H.K. Sarmah : MHD Transient flow past an impulsively started infinite horizontal porous plate in a rotating system with hall current: Int J. of Appl. Math and Mech. 7(2), (2011), pp 1-15.

2. Anwar Beg, O,Joaquin Zueco and Takhar,H.S:Unsteady magneto-hydrodynamic Hartmann-Couette flow and heat transfer in a Darcian channel with hall currents, ionslip, Viscous and Joule heating:Network Numerical solutions,Commun Nonlinear Sci Numer Simulat,V.14, (2009),pp.1082-1097 .

3. Cheng-Yang Cheng, Combined heat and mass transfer in natural convection flow from a vertical wavy surface in a power-law fluid saturated porous medium with thermal and mass stratification. Int. Commun. Heat and Mass transfer 36, (2009),pp. 351-356.

4. Debnath,L:Exact solutions of unsteady hydrodynamic and hydromagnetic boundary layer equations in a rotating fluid system, ZAMM, V.55, (1975), pp.431.

5. Debnath,L:ZAMM.V.59, (1979),pp.469-471.

6. Krishna,D.V, Prasada rao,D.R.V, Ramachandra Murty,A.S:Hydromagnetic convection flow through a porous medium in a rotating channel., J.Engg. Phy. and Thermo.Phy,V.75(2),pp.281-291.

7. Kumar H : Heat Transfer with radiation and temperature dependent heat source in MHD Free convection flow confined between two vertical wavy walls. Int.J. of Appl. Math and Mech. 7 (2),(2011), pp 77-103,

8. Mahdy A, Mohamed R.A, and Hady F.M.: Natural Convection Heat and Mass Transfer over a vertical wavy surface with variable wall temperature and concentration in porous media: Int.J. of Appl. Math and Mech. 7(3), (2011),pp. 1-13.

9. Naga Leela Kumari : Effect of Hall current on the convective heat and mass transfer flow of a viscous fluid in a horizontal channel presented at APSMS conference, SBIT, Khammam, (2011).

10. Pop,I:J.Maths.Phys.Sci.,V.5,(1971),pp.375.

11. Rao,D.R.V,Krishna,D.V and Debnath,L:Combined effect of free and forced convection on MHD flow in a rotating porous channel, Int. J. Maths and Math. Sci,V.5, (1982),pp.165-182.

12. Rajesh Yadav Y , Rama Krishna S and Reddaiah P : Mixed Convective Heat transfer through a porous medium in a Horizontal wavy channel. Int. J. of Appl. Math and Mech. 6(17),pp.25-54.

13. Rathish Kumar B.V., Shalini Gupta. : Combined influence of mass and thermal stratification on double diffusion non-Darcian natural convection form a wavy vertical channel to porous media, ASME J. Heat Transfer 127,(2005),pp. 637-647.

14. Rees. D.A.S., Pop. I. : A note on free convection along a vertical wavy surface in a porous medium. ASME J. Heat Transfer 116, (1994),pp.505-508.

15. Rees. D.A.S., Pop. I. : Free convection induced by a vertical wavy surface with uniform heat flux in a porous medium, ASME J. Heat Transfer 117 (1995),pp. 547-550.

16. Sarkar,D Mukherjee,S:Acta Ciencia Indica.,V.34M,No.2, (2008),pp.737-751.

17. Sato,H:J.Phy.Soc.,Japan,V.16, (1961),pp.1427.

18. Seth,G.S,Ansari,S and Ahmad,N : Acta Ciencia Indica ,V.34M, No.4,(2008),pp.1849.

19. Seth,G.S,Ansari,S,Mahto,N and Singh,S.K :Acta ciencia Indica, V.34M. No.3, (2008),pp.1279- 1288.

20. Shalini, B.V. Rathish Kumar, Influence of variable heat flux on natural convection along a corrugated wall in porous media, Commun. Non-linear Sci. Numer. Simul. 12, (2007),pp.1454-1463.

21. Shanti G: Hall effects on convective heat and mass transfer flow of a viscous fluid in a vertical wavy channel with Oscillatory flux and radiation, J. Phys and Appl.Phys,V.22, (2010),No.4.

22. Sherman,A and Sutton,G.W: MHD ,Evanston,Illionis, (1961),pp.173.

23. Sivaprasad, R, Prasada Rao, D.R.V and Krishna,D.V: Hall effects on unsteady MHD free and forced convection flow in a porous rotating channel., Ind.J. Pure and Appl.Maths,V.19(2),(1988),pp.688-696.

24. Yamanishi,T: Hall effects on hydromagnetic flow between two parallel plates.,Phy.Soc.,Japan,Osaka,V.5,(1962),pp.29.